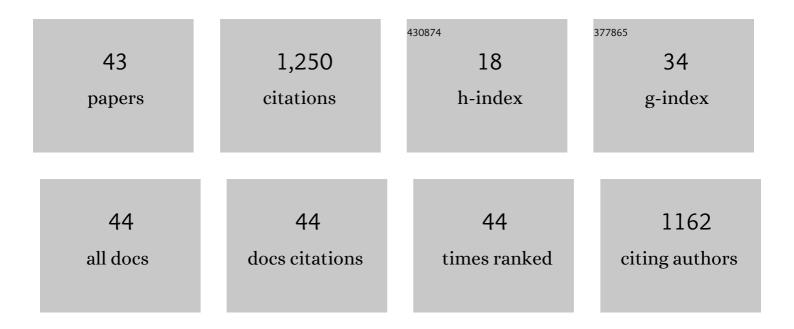
Hai-You Huang

List of Publications by Year in descending order

Source: https://exaly.com/author-pdf/3736796/publications.pdf Version: 2024-02-01



#	Article	IF	CITATIONS
1	Growth and Photocatalytic Activity of Dendrite-like ZnO@Ag Heterostructure Nanocrystals. Crystal Growth and Design, 2009, 9, 3278-3285.	3.0	206
2	SESF-Fuse: an unsupervised deep model for multi-focus image fusion. Neural Computing and Applications, 2021, 33, 5793-5804.	5.6	112
3	Giant elastocaloric effect covering wide temperature range in columnar-grained Cu _{71.5} Al _{17.5} Mn ₁₁ shape memory alloy. APL Materials, 2016, 4, 106106.	5.1	79
4	The roles of grain orientation and grain boundary characteristics in the enhanced superelasticity of Cu71.8Al17.8Mn10.4 shape memory alloys. Materials & Design, 2014, 64, 427-433.	5.1	78
5	Superelastic anisotropy characteristics of columnar-grained Cu–Al–Mn shape memory alloys and its potential applications. Materials and Design, 2015, 85, 211-220.	7.0	68
6	Deep Learning-Based Image Segmentation for Al-La Alloy Microscopic Images. Symmetry, 2018, 10, 107.	2.2	62
7	Machine learning assisted design of γ′-strengthened Co-base superalloys with multi-performance optimization. Npj Computational Materials, 2020, 6, .	8.7	56
8	Structure design of high-performance Cu-based shape memory alloys. Rare Metals, 2015, 34, 607-624.	7.1	44
9	Interfacial Microstructure and Bonding Strength of Copper Cladding Aluminum Rods Fabricated by Horizontal Core-Filling Continuous Casting. Metallurgical and Materials Transactions A: Physical Metallurgy and Materials Science, 2011, 42, 4088-4099.	2.2	42
10	Data augmentation in microscopic images for material data mining. Npj Computational Materials, 2020, 6, .	8.7	41
11	Tuning the operation temperature window of the elastocaloric effect in Cu–Al–Mn shape memory alloys by composition design. Journal of Alloys and Compounds, 2020, 828, 154265.	5.5	36
12	Effects of Processing Parameters on the Fabrication of Copper Cladding Aluminum Rods by Horizontal Core-Filling Continuous Casting. Metallurgical and Materials Transactions B: Process Metallurgy and Materials Processing Science, 2011, 42, 104-113.	2.1	32
13	Texture evolution and flow stress of columnar-grained polycrystalline copper during intense plastic deformation process at room temperature. Materials Science & Engineering A: Structural Materials: Properties, Microstructure and Processing, 2011, 530, 418-425.	5.6	30
14	Superelastic fatigue of columnar-grained Cu-Al-Mn shape memory alloy under cyclic tension at high strain. Scripta Materialia, 2017, 136, 106-110.	5.2	30
15	Microstructure and superelasticity control by rolling and heat treatment in columnar-grained Cu-Al-Mn shape memory alloy. Materials Science & Engineering A: Structural Materials: Properties, Microstructure and Processing, 2017, 696, 315-322.	5.6	29
16	Tuning the Ferroelectric and Piezoelectric Properties of 0.91Pb(Zn1/3Nb2/3)O3-0.09PbTiO3 Single Crystals and Lead Zirconate Titanate Ceramics by Doping Hydrogen. Journal of Physical Chemistry C, 2010, 114, 9955-9960.	3.1	21
17	Effects of aging treatment on the microstructure and superelasticity of columnar-grained Cu71Al18Mn11 shape memory alloy. International Journal of Minerals, Metallurgy and Materials, 2016, 23, 1157-1166.	4.9	20
18	Effects of Strain Rate and Measuring Temperature on the Elastocaloric Cooling in a Columnar-Grained Cu71Al17.5Mn11.5 Shape Memory Alloy. Metals, 2017, 7, 527.	2.3	20

HAI-YOU HUANG

#	Article	IF	CITATIONS
19	Enhanced room-temperature tensile ductility of columnar-grained polycrystalline Cu–12wt.%Al alloy through texture control by Ohno continuous casting process. Materials Letters, 2011, 65, 1123-1126.	2.6	19
20	Accelerating the development of multi-component Cu-Al-based shape memory alloys with high elastocaloric property by machine learning. Computational Materials Science, 2020, 176, 109521.	3.0	19
21	Numerical simulation of temperature field in horizontal core-filling continuous casting for copper cladding aluminum rods. International Journal of Minerals, Metallurgy and Materials, 2013, 20, 684-692.	4.9	18
22	Deep learningâ€based automatic inpainting for material microscopic images. Journal of Microscopy, 2021, 281, 177-189.	1.8	17
23	Microbridge tests on gallium nitride thin films. Journal of Micromechanics and Microengineering, 2009, 19, 095019.	2.6	15
24	Dynamic Recovery and Superelasticity of Columnar-Grained Cu–Al–Mn Shape Memory Alloy. Metals, 2017, 7, 141.	2.3	15
25	An infrastructure with user-centered presentation data model for integrated management of materials data and services. Npj Computational Materials, 2021, 7, .	8.7	15
26	Two-Way Shape Memory Effect Induced by Tensile Deformation in Columnar-Grained Cu71.7Al18.1Mn10.2 Alloy. Materials, 2018, 11, 2109.	2.9	11
27	Large [001] single crystals via abnormal grain growth from columnar polycrystal. Materialia, 2019, 6, 100336.	2.7	11
28	A fast algorithm for material image sequential stitching. Computational Materials Science, 2019, 158, 1-13.	3.0	11
29	Effect of strain rate on the compressive deformation behaviors of lotus-type porous copper. International Journal of Minerals, Metallurgy and Materials, 2014, 21, 687-695.	4.9	10
30	Stress-induced phase transformation characteristics and its effect on the enhanced ductility in continuous columnar-grained polycrystalline Cu–12wt%Al alloy. Materials Science & Engineering A: Structural Materials: Properties, Microstructure and Processing, 2014, 596, 103-111.	5.6	10
31	The behaviour of 180° polarization switching in BaTiO3 from first principles calculations. Computational Materials Science, 2014, 82, 1-4.	3.0	10
32	Fine-tuning the ductile-brittle transition temperature of Mg2Si intermetallic compound via Al doping. International Journal of Minerals, Metallurgy and Materials, 2019, 26, 507-515.	4.9	10
33	Effect of compression direction on the dynamic recrystallization behavior of continuous columnar-grained CuNi10Fe1Mn alloy. International Journal of Minerals, Metallurgy and Materials, 2015, 22, 851-859.	4.9	8
34	Machine learning assisted empirical formula augmentation. Materials and Design, 2021, 210, 110037.	7.0	8
35	Experiments and first principles calculations on the effects of hydrogen on the optical properties of ferroelectric materials. Journal of Materials Science, 2009, 44, 5768-5772.	3.7	7
36	DO22–(Cu,Ni)3Sn intermetallic compound nanolayer formed in Cu/Sn-nanolayer/Ni structures. Journal of Alloys and Compounds, 2009, 486, 207-211.	5.5	7

HAI-YOU HUANG

#	Article	lF	CITATIONS
37	Tension–compression asymmetry of stress-induced transformations in martensitic Cu-12wt.% Al alloys. Materials Letters, 2012, 79, 51-54.	2.6	7
38	Fracture criterion for conductive cracks in soda-lime glass under combined mechanical and electrical loading. International Journal of Fracture, 2010, 164, 185-199.	2.2	5
39	Cu diffusion kinetics in (Cu, Ni)3Sn intermetallic compound nanolayers investigated by an Energy-Dispersive-X-ray-based permeation test. Thin Solid Films, 2009, 518, 201-205.	1.8	4
40	Stress relaxation behavior of columnar-grained Cu–Al–Mn shape memory alloys. Materials Science & Engineering A: Structural Materials: Properties, Microstructure and Processing, 2019, 768, 138432.	5.6	3
41	First principles calculations of hydrogen-induced decrease in the cohesive strength of α-Al2O3 single crystals. Computational Materials Science, 2012, 54, 81-83.	3.0	2
42	Hydrogen in Ferroelectrics. , 0, , .		1
43	Effect of Alloying Elements on the Stacking Fault Energy and Ductility in Mg ₂ Si Intermetallic Compounds. ACS Omega, 2021, 6, 20254-20263.	3.5	1